Quantum Yield Switching of Fluorescence by Selectively Bridging Single and Double Bonds in Chalcones: Involvement of Two Different Types of Conical Intersections

Knut Rurack,[†,‡] Marina L. Dekhtyar,[§] Julia L. Bricks,[§] Ute Resch-Genger,[‡] and Wolfgang Rettig*[,†]

Institut für Physikalische und Theoretische Chemie, Humboldt Universität zu Berlin, Bunsenstr. 1, D-10117 Berlin, Germany, Bundesanstalt für Materialforschung und -prüfung (BAM), Richard-Willstätter-Str. 11, D-12489 Berlin, Germany, and Institute of Organic Chemistry, National Academy of Sciences of the Ukraine, Murmanskaya 5, 253660, Kiev-94, Ukraine

Received: August 13, 1999; In Final Form: October 1, 1999

From the fluorescence properties of chalcones as a function of solvent polarity, and by the comparison to derivatives with donors and acceptors and with various selectively bridged bonds, it can be concluded that two emissive and two nonemissive states are needed to describe the fluorescence behavior. Three of these states are connected with bond twisting and lead to species with high or low dipole moment, two of them situated in the proximity of a conical intersection.

1. Introduction

The photophysical properties of chalcones have been studied by numerous researchers[1−7] since this class of dyes has been widely used for various optical applications including nonlinear optical materials for second harmonic generation,[8] photorefractive polymers,[9] holographic recording technology,[10] and fluorescent probes for the sensing of metal ions[11] or the microenvironment in micelles.[6] Whereas most 4,4′-substituted chalcones absorb in the UV spectral region and are weakly fluorescent or nonfluorescent in solvents of small or large polarity,[5] 4′-(dimethylamino)chalcone **1** (Scheme 1) shows a strongly solvatochromic emission behavior and a reasonable fluorescence quantum yield in polar aprotic solvents.[6,7]

The results obtained during our studies on related fluoroionophores, i.e., monoaza crown ether substituted heteroaromatic analog of **1**,[11,12] have led us to a more detailed investigation of the excited state processes governing the emission behavior of chalcones and including the derivatives **1**−**4** (Scheme 1). Furthermore, the findings reported by Wang[3] and Wang and Wu[7] on the spectroscopic properties of the (partly or fully) bridged compounds **5**−**8** (Scheme 1) suggested that a simple reaction model involving only one photochemical funnel does not sufficiently describe the deactivation of photoexcited 4′-(dimethylamino)chalcones. But especially for applicational purposes such as metal ion or environmental sensing, it would be most helpful to be able to answer the question, how can molecular bridging achieve fluorescence enhancement in a given chromophore?

The original idea of bridging was connected with the loose bolt theory[13] which states that flexible groups or substituents behave like a loose bolt causing the preference of nonradiative decay pathways to the ground state and therefore causing fluorescence quenching. Some well-known examples of successful fluorescence enhancement are the bridged rhodamine 101[14] and the bridged coumarin 102.[15] However, when other compounds with similar large flexible substituents are compared, differences in fluorescence efficiency of several orders of magnitude can be encountered which cannot be explained by the loose bolt theory. For example, a few cases have been described where bridging of flexible groups results in the opposite effect, namely lowering of the fluorescence quantum yields.[16−19] This initiated the search for an adiabatic photochemical mechanism which can explain the fluorescence losses.

SCHEME 1: Chemical Structures of the Chalcone Derivatives Studied; 1−4, 1-Cl, 1-OMe, 2-Cl, and 2-OMe Have Been Experimentally Investigated in This Work, 5−8 Were Described in refs 3 and 7

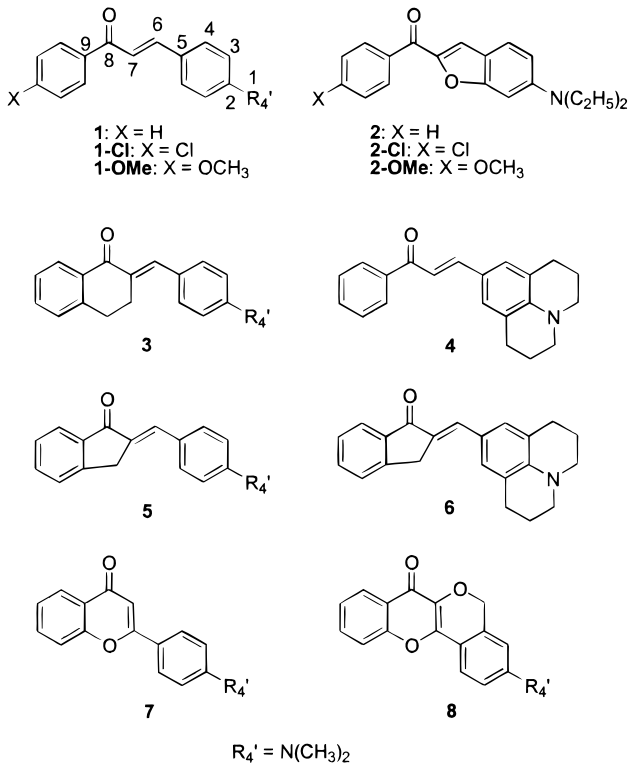

[†] Institut für Physikalische und Theoretische Chemie.
[‡] Bundesanstalt für Materialforschung und -prüfung.
[§] Institute of Organic Chemistry.

10.1021/jp992878m CCC: $18.00
Published on Web 11/12/1999

In a comparison of differently bridged triphenylmethane,[20] rhodamine,[21] and other xanthene dyes,[22,23] arguments were given for a simultaneous involvement of a twisting relaxation and a charge-transfer interaction. This mechanism could explain the 500-fold weaker fluorescence quantum yield for a rhodamine derivative[23] where the usual acceptor carboxylic ester was replaced by an amino donor group, as well as the restoring of the large fluorescence quantum yield through protonation which causes an increase of the loose bolt character but eliminates the strong donor group. Such an "anti-loose bolt behavior" has also been observed in connection with molecular bridging, e.g., for a series of donor−acceptor-substituted stilbenes (D−A−stilbenes),[16,17] indicating that not the flexibility or rigidity alone is the decisive factor but that further adiabatically formed excited-state product species may be involved and can have intrinsic fluorescence properties depending on the specific case considered. This photochemical mechanism of fluorescence quenching or enhancement is closely related to the so-called twisted intramolecular charge transfer (TICT) states (for reviews see ref 24). With this in mind, we extended the series of selectively bridged chalcones of varying donor and acceptor strength by the synthesis of **1-Cl**, **1-OMe**, **2**, **2-Cl**, **2-OMe**, **3**, and **4** (Scheme 1).

The experimental part of this work comprises steady state absorption and fluorescence measurements of **1**, **1-Cl**, **1-OMe**, **2**, **2-Cl**, **2-OMe**, **3**, and **4**, where the study of the first compound was done for a better comparison with the data published so far. The quantum chemical calculations were performed in order to elucidate theoretically the role of excited state bond rotation on the relative energies of ground and the different types of excited states. The aim of this paper is to analyze the mechanism of bond rotation and its influence on the photophysics of chalcones.

2. Experimental and Calculations

Materials. All solvents were of UV spectroscopic grade and were purchased from Aldrich. For the syntheses, starting materials from Lancaster and Aldrich were used.

Apparatus. The chemical structures of the synthesized compounds were confirmed by elemental analysis, ^{1}H NMR, and ^{13}C NMR. Their purity was checked by reversed phase HPLC (HPLC set up from Merck-Hitachi; RP18 column; acetonitrile/water = 75:25 as eluent) employing UV detection (UV detector from Knaur; fixed wavelength at 310 nm). Melting points (uncorrected) were measured with a digital melting point analyzer IA 9100 (Kleinfeld GmbH) and NMR spectra were obtained with a 500 MHz NMR spectrometer Varian Unity$_{plus}$ 500.

Spectroscopy. The steady-state measurements were performed on a SPECORD M400/M500 spectrophotometer from Carl Zeiss Jena and a Spectronics Instruments 8100 spectrofluorometer. For the fluorescence experiments, only dilute solutions with an optical density (OD) below 0.01 at the excitation wavelength (OD < 0.04 at the absorption maximum) to avoid reabsorption in the case of small Stokes shifts were used. The relative fluorescence quantum yields (ϕ_f) were determined by adjusting the optical densities of the solutions at the excitation wavelengths to 0.1 ± 0.001 in a 100 mm absorption cell. These solutions were then transferred to a 10 mm quartz cell, and the fluorescence measurements were performed with a 90° standard geometry and an emission polarizer set at 54.7°. All fluorescence spectra presented here are corrected for the spectral response of the detection system (calibrated quartz halogen lamp placed inside an integrating sphere; Gigahertz-Optik) and for the spectral irradiance of the excitation channel (calibrated silicon diode mounted at a sphere port; Gigahertz-Optik). The fluorescence quantum yields were calculated from six independent measurements according to eq 1 employing the fluorescence standards coumarin 102 (ϕ_f = 0.6 in ethanol) and coumarin 153 (ϕ_f = 0.4 in ethanol)[25] and the uncertainties of the measurement were determined to ±10% (for $\phi_f > 0.02$), ±20% (for $0.02 > \phi_f > 5 \times 10^{-3}$), and ±30% (for $5 \times 10^{-3} > \phi_f$), respectively.

$$\phi_f^i = \phi_f^s \frac{A_s}{A_i} \frac{I_f^i(\lambda)}{I_f^s(\lambda)} \frac{{n_i}^2}{{n_s}^2} \quad (1)$$

Here, the subscripts i and s denote the quantities of unknown compound and standard, A_x is the absorption at the excitation wavelength, $I_f^x(\lambda)$ is the integrated fluorescence intensity, and n_x is the refractive index of the solvent.

Trans−cis isomerization experiments were performed employing a unique laser impulse fluorometer described elsewhere.[26] The sample was excited with the second harmonic output (LBO crystal) of a regenerative mode-locked argon ion laser-pumped Ti:sapphire laser at a repetition rate of 82 MHz. The fluorescence was collected at right angles (polarizer set at 54.7°; monochromator with spectral bandwidths of 8 nm) and the fluorescence spectra were recorded with a modified time-correlated single photon counting setup. The laser beam was attenuated using a double prism attenuator from LTB and excitation energies were in the nanowatt to milliwatt range (average laser power). The excitation energies were checked and adjusted with a calibrated Si diode (model 221 with 100:1 attenuator 2550, Graseby) and an optometer (model S370, Graseby).

Syntheses. 1, 3-(4-(dimethylamino)phenyl)-1-phenylprop-2-en-1-one,[27] **1-OMe**,[28] and **1-Cl**[29] were synthesized by reacting the (substituted) acetophenone precursor with the corresponding 4-substituted benzaldehyde derivative following a procedure described previously.[30] For the synthesis of **2**, **2-OMe**, and **2-Cl**, a mixture of 4-diethylaminosalicylaldehyde (1 mmol), the corresponding bromoacetophenone (2.6 mmol), potassium carbonate (0.137 g), and tetrabutylammonium hydrogen sulfate (0.137 g) in 14 mL dimethylacetamide was heated for 4 h at 100−105 °C. After cooling, the resulting mixture was poured into 75 mL water and extracted with toluene (3 × 75 mL). The extract was dried over $MgSO_4$ and evaporated. The final product was purified twice by column chromatography on silica gel (toluene/ethyl acetate 1:1 and cyclohexane/ethyl acetate 1:1) and crystallized from hexane.

*(6-Diethylaminobenzofuran-2-yl)phenylmethanone (**2**).* Yield: 68%. Dark-yellow needles, mp 76−77 °C. Calculated for $C_{19}H_{19}NO_2$: C 77.77, H 6.53, N 4.78. Found: C 77.56, 77.48; H 6.45, 6.47; N 4.64, 4.68. ^{1}H NMR ($CDCl_3$) δ (ppm): 1.200−1.246 (t, J = 7 Hz, 6H), 3.405−3.475 (q, J = 7.1 Hz, 4H), 6.740−6.771 (dd, J_1 = 2.4 Hz, J_2 = 8.8 Hz, 1H), 6.769−6.777 (d, J = 2.4 Hz, 1H), 7.381−7.384 (d, J = 0.8 Hz, 1H), 7.456−7.608 (m, 4H), 7.950−7.982 (m, 2H). ^{13}C NMR ($CDCl_3$) δ (ppm): 12.479; 45.021; 92.805; 111.077; 116.263; 118.481; 123.659; 128.313; 129.093; 132.035; 138.201; 149.391; 150.244; 159.312; 183.397.

*(6-Diethylaminobenzofuran-2-yl)(4-chlorophenyl)methanone (**2-Cl**).* Yield: 52%. Dark-yellow crystals, mp 98−100 °C. Calculated for $C_{19}H_{18}ClNO_2$: C 69.61, H 5.53, N 4.27. Found: C 69.54, 69.59; H 5.63, 5.70; N 4.33, 4.34. ^{1}H NMR ($CDCl_3$) δ (ppm): 1.213−1.241 (t, J = 7.0 Hz, 6H), 3.423−3.465 (q, J = 7.0 Hz, 4H), 6.759−6.773 (broad, 2H), 7.394 (s,

1H), 7.470−7.487 and 7.935−7.952 (dd, J = 8.4 Hz, 4H), 7.473−7.491 (d, J = 9.0 Hz, 1H). ^{13}C NMR ($CDCl_3$) δ (ppm): 12.450; 45.038; 92.686; 111.249; 116.182; 118.404; 123.752; 128.647; 129.106; 129.769; 130.593; 136.392; 138.425; 149.535; 150.089; 159.312; 181.854.

*(6-Diethylaminobenzofuran-2-yl)(4-methoxyphenyl)methanone (**2-OMe**).* Yield: 51%. Yellow needles, mp 97−99 °C. Calculated for $C_{20}H_{21}NO_3$: C 74.28, H 6.55, N 4.33. Found: C 74.11, 74.24; H 6.60, 6.67; N 4.35, 4.44. ^{1}H NMR ($CDCl_3$) δ (ppm): 1.198−1.245 (t, J = 7.0 Hz, 6H), 3.402−3.473 (q, J = 7.1 Hz, 4H), 3.895 (s, 3H), 6.744 (broad, 1H), 6.778 (broad, 1H), 6.972−7.020 (m, 2H), 7.389 (s, 1H), 7.459−7.488 (d, J = 8.7 Hz, 1H), 8.020−8.049 (d, J = 8.8 Hz, 2H). ^{13}C NMR ($CDCl_3$) δ (ppm): 12.479; 45.005; 55.447; 92.917; 110.949; 113.618; 116.295; 117.348; 123.474; 130.733; 131.456; 149.142; 150.613; 159.046; 162.937; 182.094.

3 was synthesized according to a method described in ref 31. For **4**, a similar strategy as for **1** was employed and the synthesis of 7-formyljulolidine was described in ref 32. A solution of 0.18 g (1.5 mmol) acetophenone and 0.301 g (1.5 mmol) 7-formyljulolidine in 0.5 mL 2 N aqueous NaOH was refluxed for 3 min and stirred at room temperature for 20 h. Water (50 mL) was added and the mixture was extracted with toluene (3 × 50 mL). The organic layer was dried ($MgSO_4$) and concentrated under reduced pressure to give a yellow oil (0.38 g). Purification by column chromatography (silica gel, toluene) yielded crystalline **4**.

*1-Phenyl-3-(2,3,6,7-tetrahydro-1H,5H-benzo[i,j]quinolizin-7-yl)-2-propen-1-one (**4**).* Yield: 61.5%. Red needles, mp 123−125 °C (from *n*-hexane). Calculated for $C_{21}H_{21}NO$: C 83.13, H 6.98, N 4.62. Found: C 82.98, 83.02; H 7.05, 7.12; N 4.75, 4.78. ^{1}H NMR ($CDCl_3$) δ (ppm): 1.944−1.992 (m, 4H), 2.746−2.772 (t, J = 6.4 Hz, 4H), 3.236−3.259 (t, J = 5.8 Hz, 4H), 7.110 (s, 2H), 7.244−7.274 and 7.689−7.719 (2 × d, J = 15.3 Hz, 2H), 7.453−7.482 (m, 2H), 7.515−7.544 (t, J = 7.3 Hz, 1H), 7.979−7.998 (d, J = 7.9 Hz, 2H). ^{13}C NMR ($CDCl_3$) δ (ppm): 21.380, 27.592, 50.156, 111.730, 116.852. 122.555, 128.214, 128.338, 130.310, 132.023, 138.992, 145.741, 151.940, 190.590.

Quantum Chemical Calculations. AM1 calculations[33] using the AMPAC package[34] were performed to yield the ground state and excited state energies for various conformations of **1**−**8**. In the course of the ground-state energy calculations for the 90°-twisted conformations of **1**, the structures were fully optimized except for a single dihedral angle fixed at 90° and associated with the corresponding twisted bond. The energies of the excited states were calculated for the rigidized ground state geometry, with eight molecular orbitals involved in the configuration interaction including 200 single and multiple excitations. The effect of solvent stabilization for the ground and the excited states was calculated similar as in ref 35, on the basis of the Onsager model.[36,37] In the determination of the Onsager cavity parameter by the mass−density formula,[38] the density of **1** (with the molar mass of 257 g) was taken to be equal to that of dimethylaniline (0.95 g cm^{-3}). The dielectric constant of acetonitrile was taken as 37.5.

3. Results

Absorption and Fluorescence Spectroscopy. *Steady-State Spectra and Solvatochromism.* The absorption and fluorescence spectra of **1**−**4** in solvents of different polarity are shown in Figure 1, and selected spectroscopic data of **1**−**8**, **1-Cl**, **1-OMe**, **2-Cl**, and **2-OMe** are included in Table 1. For **1**−**4, 1-Cl**, **1-OMe**, **2-Cl**, and **2-OMe**, the absorption and fluorescence

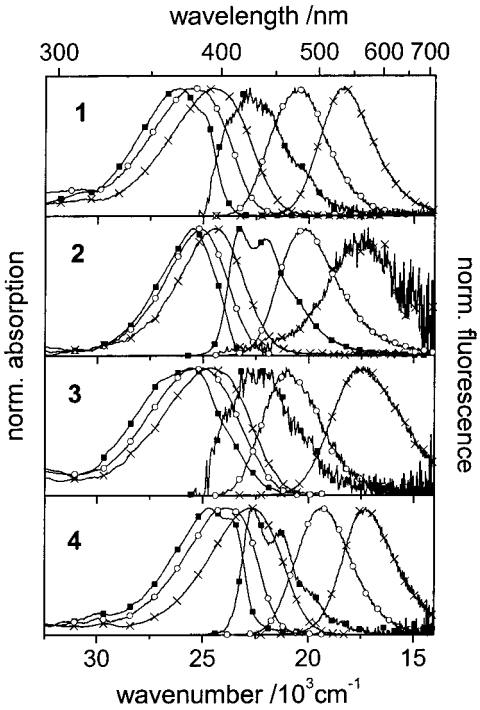

Figure 1. Normalized steady-state absorption and emission spectra of **1**, **2**, **3**, and **4** in *n*-hexane (solid squares), diethyl ether (open circles), and acetonitrile (crosses) at room temperature.

excitation spectra match and no different behavior has been reported for **5**−**8**. The intramolecular charge transfer (ICT) character of all 12 donor−acceptor-substituted chalcones (D−A−chalcones) is characterized by an increase in Stokes shift with increasing solvent polarity pointing to a stronger stabilization of the excited state in polar solvents. Consequently, the excitation of the ICT state involves a charge shift from the dimethylanilino (DMA) donor to the carbonyl−phenyl (COPh) acceptor fragment, and the dipole moment of the resultant excited state (μ_{es}) is larger than that of the ground state ($\mu_{es} > \mu_{gs}$). Analyzing the solvatochromic data according to the Bilot−Kawski formalism by a plot of the Stokes shift vs BK (eq 2[39]), Wang and Wu determined ($\mu_{es} - \mu_{gs}$) to be 5.9, 5.6, 8.2, and 5.8 D for **1**, **5**, **7**, and **8**, respectively.[7] In another paper, Wang found a value of ($\mu_{es} - \mu_{gs}$) = 10 D for **5** on the basis of correlating the absorption maxima in different solvents according to a method proposed by Varma and Groenen.[3,40] In the present work, again the BK formalism taking into account the polarizability of the solute was employed, and the change in dipole moment was calculated from the slope of a plot according to eq 2.

$$\Delta\tilde{\nu}(\text{abs}-\text{em}) = \Delta\tilde{\nu}^{\text{vac}}(\text{abs}-\text{em}) + \frac{2(\mu_{es}-\mu_{gs})^2}{hc_0a_O{}^3}BK \quad (2)$$

with

$$BK = \left(\frac{f(\epsilon_r) - f(n)}{(1-\beta f(n))^2(1-\beta f(\epsilon_r))}\right), \quad f(\epsilon_r) = \frac{\epsilon_r - 1}{2\epsilon_r + 1},$$

$$\text{and } f(n) = \frac{n^2-1}{2n^2+1}$$

In eq 2, h is Planck's constant, c_0 is the speed of light in a vacuum, ϵ_r and n are the dielectric constant and refractive index of the solvent, and $\beta = 2\alpha/a_O{}^3$ is a polarizability term including

TABLE 1: Spectroscopic Data of 1−8, 1-Cl, 1-OMe, 2-Cl, and 2-OMe in Selected Solvents (Second Maxima Are Given in Brackets[a])

	n-hexane			diethyl ether			acetonitrile		
	$\tilde{\nu}$ (abs) 10^3 cm^{-1}	$\tilde{\nu}$ (em) 10^3 cm^{-1}	ϕ_f	$\tilde{\nu}$ (abs) 10^3 cm^{-1}	$\tilde{\nu}$ (em) 10^3 cm^{-1}	ϕ_f	$\tilde{\nu}$ (abs) 10^3 cm^{-1}	$\tilde{\nu}$ (em) 10^3 cm^{-1}	ϕ_f
1	26.4 (25.1)	22.8 (23.9)	1×10^{-4}	25.3	20.6	0.02	24.4	18.4	0.15
2	26.1 (24.9)	23.3 (21.9)	0.046	25.1	20.3	0.051	24.5	17.6	1×10^{-3}
3	26.7 (25.2)	21.9 (23.4)	7×10^{-5}	25.6	20.9	2×10^{-3}	24.7	17.4	0.027
4	24.9 (23.6)	22.6 (21.3)	3×10^{-3}	23.8	19.3	0.14	22.7	17.3	0.015
5[b]	25.6[c]	24.1	1×10^{-4}	24.7[d]	21.8	7×10^{-3}	24.0	18.7[e]	0.045[e]
6[b]	26.0	22.8	0.011	n.r.[f]	20.5	0.024	24.5	18.2	5×10^{-3}
7[e]	28.6	n.r.	7×10^{-3}	n.r.	23.9	0.87	26.8	21.1	1
8[e]	n.r.	n.r.	0.50	n.r.	22.4	1	25.2	20.4	0.86
1-Cl	26.0 (24.6)	23.3 (21.8)	4×10^{-4}	24.8	20.0	0.059	24.0	17.8	0.094
1-OMe	26.7 (25.4)	22.2 (23.9)	2×10^{-4}	25.7	20.9	0.013	24.7	19.0	0.18
2-Cl	25.3 (24.1)	22.8 (21.5)	0.11	24.6	19.7	0.036	24.1	16.9	2×10^{-3}
2-OMe	26.1 (25.0)	23.8 (22.5)	0.02	25.3	20.5	0.18	24.6	18.3	0.013

[a] Low-energy absorption band fitted to a progression of $j = 4$ gaussian bands. [b] Taken from ref 3. [c] Mean value of two maxima at 26.2 and 25.1 (spectra not shown), taken from ref 3. [d] Mean value of two maxima at 25.1 and 24.4 (spectra not shown), taken from ref 3. [e] Taken from ref 7. [f] Not reported.

TABLE 2: Dipole Moments of 1−4, 1-Cl, 1-OMe, 2-Cl, and 2-OMe Obtained from the Slope of Solvatochromic Plots According to Eq 2

	a_O[a] Å	μ_{gs}[b] D	slope	$(\mu_{es}-\mu_{gs})$ D
1	5.7	3.9	3160	7.6
2	5.7	4.7	4770	9.4
3	5.7	3.9	3840	8.4
4	5.7	4.6	3810	8.4
1-Cl	5.9	4.1	3740	8.7
1-OMe	6.6	2.7	2750	8.9
2-Cl	5.9	4.8	5180	10.3
2-OMe	6.6	3.7	4450	11.3

[a] Determined on the basis of the AM1 optimized ground state geometry according to a method proposed by Lippert[68] for elongated molecules. [b] Calculated for optimized ground state geometry by AM1.

the solute polarizability α and the Onsager cavity radius a_O ($\alpha/a_O^3 \cong 0.5$ for the isotropic polarizability). The values of $(\mu_{es} - \mu_{gs})$ obtained for the chalcones studied in this work are collected in Table 2. Apart from the crucial choice of the correct Onsager cavity radius, the different values agree well for the molecules **1**, **2**, and **3** and give further support to the fact that selective bridging of different bonds in the D−A−chalcones influences the polar CT character of the emissive state(s) only to a minor extent. The increase in acceptor strength from **1-OMe** via **1** to **1-Cl** and **2-OMe** via **2** to **2-Cl** is well documented by an increase in the slope of the corresponding solvatochromic plots (Table 2). The dependence of the spectral band positions on the strength of the ICT interaction is further exemplified by a good correlation of the absorption band maximum (cf. Table 1) and the Hammett constant σ_p (Cl, 0.23; H, 0.00; OCH_3, −0.27[41]) in a polar solvent such as, for instance, in acetonitrile. The constant σ_p is a measure for the electronic effect (of both inductive and resonance components) of the substituent in the para position.[41]

Fluorescence Quantum Yields and Solvatokinetics. In contrast, for all the compounds, the fluorescence quantum yield (ϕ_f) strongly depends on all three parameters, i.e., the bridging pattern, donor and/or acceptor strength, and the solvent polarity. Plots of ϕ_f vs $E_T(N)$, Dimroth's empirical solvent polarity scale,[42] are depicted in Figures 2 and 3. The lines in these figures, although they are only guides to the eye, indicate an opposing behavior concerning the solvent polarity dependence of the fluorescence quantum yields for the different compounds. A reduction in solvent polarity strongly enhances the fluorescence quantum yield of **2** and **2-Cl** but leads to a loss in fluorescence intensity for **1-OMe**, **3**, and **5**. A maximum in such a plot is

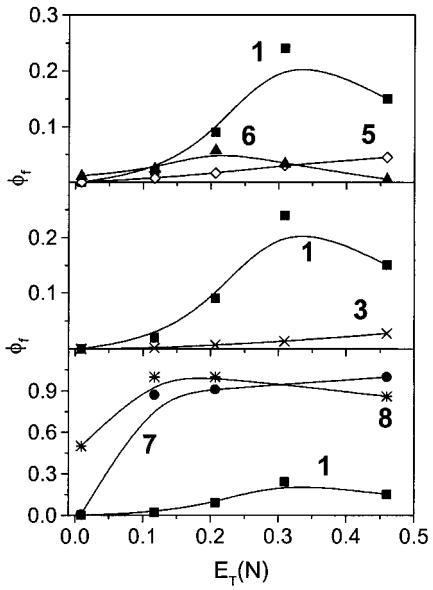

Figure 2. Plots of ϕ_f vs $E_T(N)$ for the D−A−chalcones investigated. From top to bottom: **1** (solid squares), **5** (open diamonds), and **6** (solid triangles); **1** (solid squares) and **3** (crosses); **1** (solid squares), **7** (solid circles), and **8** (stars). **1** is included in all the plots for a better comparison. The solid lines are only guides to the eye, and data in protic solvents are omitted. Data for **5**−**8** were taken from refs 3 and 7.

observed for **1-Cl**, **2-OMe**, **4**, **6**, and, to a lesser extent, **1**. For the highly bridged compounds **7** and **8**, no pronounced polarity dependence is observed and fluorescence quenching occurs only in *n*-hexane. Interestingly, the solvent polarity dependence of **1**−**6**, **1-Cl**, **1-OMe**, **2-Cl**, and **2-OMe** can be categorized into a so-called "positive solvatokinetic behavior" with a decrease in emission yield with increasing solvent polarity resulting from enhanced excited state population of a highly polar charge transfer species with strongly nonradiative properties[43,44] or a "negative solvatokinetic behavior", i.e., an increase in fluorescence quantum yield with increasing solvent polarity indicative of population of an emissive CT state. **1**, **3**, and **5** show a strongly resembling negative solvatokinetic behavior (Figure 2) with relative fluorescence quantum yields decreasing in the order **1** > **5** > **3** (Table 1, Figure 2). Accordingly, the rigid bridging of both single bonds in the acceptor part as in **5** does not yield any fluorescence enhancement but a fluorescence loss. On the other hand, tuning of the donor or acceptor strength of a

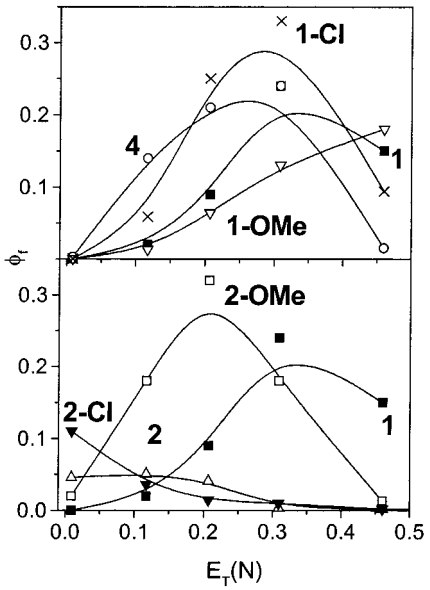

Figure 3. Plots of ϕ_f vs $E_T(N)$ for the D−A−chalcones investigated. (Top) **1** (solid squares), **1-Cl** (crosses), **1-OMe** (open triangles), and **4** (open circles); (bottom) **1** (solid squares), **2** (open triangles), **2-Cl** (solid triangles), and **2-OMe** (open squares). **1** is included in both plots for a better comparison. The solid lines are only guides to the eye and data in protic solvents are omitted.

molecule with a given bridging pattern by further substituents (**1** or **2**) can affect the solvent polarity-dependent fluorescence yield as well and enhance (**2-Cl** as compared to **2** in medium polar solvents) or reduce (**2-OMe** as compared to **2** in medium polar solvents) fluorescence losses.

Trans−Cis Isomerization. The significant occurrence of permanent trans−cis isomerization around the double bond was excluded by recording the emission spectrum of **1** as a function of laser excitation energy up to 10 mW (cw). Furthermore, HPLC analysis with UV/vis diode array detection of an irradiated sample of **1** showed only one peak, its absorption spectrum being identical to that of a reference sample kept in the dark. The same was found for all the freshly synthesized compounds **1**−**4**. Chalcone cis isomers described in the literature so far show strongly hypsochromically shifted absorption spectra and population of the short-lived species was only achieved photochemically.[1]

Quantum Chemical Calculations. *Single and Double Bond Isomerism and the Ground State Surface.* When dealing with chalcone photophysics or photochemistry, one has to be aware of a complex equilibrium involving different conformers for both isomers possibly populated already in the ground state. As depicted in Scheme 2, besides trans−cis isomerism at the central double bond b_{67}, s-cis ("*c*") and s-trans ("*t*") single bond isomerism (bond b_{78}) can occur (to avoid "cis", "trans", as well as "double bond isomer" and "*s*-isomer" misunderstandings, the double bond isomers are labeled *E* and *Z* and the single bond isomers *c* and *t*, arriving at *cE*, *tE*, *cZ*, and *tZ conformers*, as depicted in Scheme 2. Ground-state geometry optimizations for both *E* conformers converge in the case of the b_{78} unbridged compounds (for labeling see Scheme 1) yielding comparably small energy differences for both pairs of *tE* and *cE* conformers, $\Delta E(tE-cE) = 6$ kJ mol^{-1} for **1** and 2 kJ mol^{-1} for **2**, respectively. Following the Boltzmann description for the ratio of the population of two states (eq 3), values of $N(tE)/N(cE) = 0.09$ (for **1**) and 0.45 (for **3**) are obtained for $T = 298$ K.

SCHEME 2: Chemical Structures of Possible Chalcone Conformers[a]

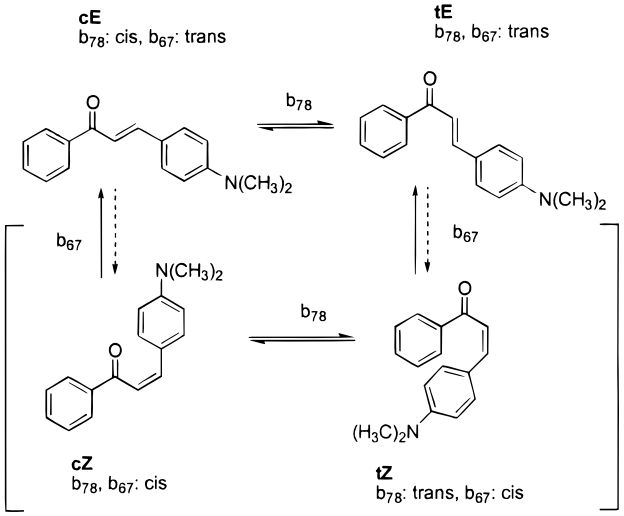

[a] The bonds affected by a 180° twist are labeled according to formula 1 in Scheme 1. In the top row, the two stable conformers of the double bond b_{67} *E* isomer and in the bottom row, the sterically unfavorable *Z* conformers are shown. The conformation of bonds b_{67} and b_{78} is indicated and the labels on the arrows denote the bonds which have to rotate for the respective transition.

$$\frac{N(tE)}{N(cE)} = e^{-[E(tE) - E(cE)]/kT} \qquad (3)$$

However, the question if only one conformation is populated in the ground state or if both conformers are already populated in S_0 and show identical spectra remains unanswered at present. The corresponding ground state dipole moments ($\Delta\mu(tE-cE) = +0.7$ D for **1** and -0.6 D for **2**) and transition energies ($\Delta E_{S0-S1}(tE-cE) = 320$ cm^{-1} for **1** and 80 cm^{-1} for **2**) are of comparable magnitude as well. Accordingly, the same is true for the dipole moments and excitation energies of the fixed *cE* (**3**, **5**, **6**) and *tE* (**7**, **8**) conformers and is supported by the experimental data collected in Table 1. Geometry optimizations for the *tZ* and *cZ* conformers (possible in **1**, **3**, **5**, and **6**) did not converge, and these conformers are found to be highly energetically unfavorable. With fixed *Z* geometries at bond b_{67}, high energy differences of >35 kJ mol^{-1} with respect to the most stable geometry are found. For instance, these differences calculated for the *cZ* and the *tZ* conformers of **1** amount to >300 kJ mol^{-1} and >900 kJ mol^{-1}, explaining the lack of an experimental detection of *Z* conformers. Thus, besides the fixed *E* conformers, for both **1** and **2** *cE* is the slightly more stable ground state conformer, but for *tE* of **1** the higher ground state dipole moment is calculated. If bond twisting is restricted by bridging, the torsional angles (and bond lengths) obtained for optimized ground state structures of *cE* and *tE* are very similar for all the D−A−chalcone derivatives in most cases (for some examples, see Table 3).

Energy barriers for twisting in the ground state were calculated by optimizing the 90° twisted structure of the bond concerned ("perp-structure"). The barrier thus calculated for twisting of the aryl acceptor moiety is generally low for **1** and **2** (ca. 15 kJ mol^{-1}). Rotation around b_{67} in the ground state is connected with the usual high activation barrier for C=C double bonds. These data should be viewed in conjunction with experimental evidence: From X-ray studies of numerous chalcones, it is known that either *cE* or *tE* conformers are preferred in certain molecules but most of the chalcones with a simple COPh acceptor were found to crystallize in *cE*.[46]

TABLE 3: Molecular Geometrical Parameters (Bond Length, *l*, and Dihedral Angle, φ) of the Stable Ground-State Structures of 1, 2, 3, and 5 as Calculated by AM1-Optimization (Bond Lengths of the *tE* Conformers Are Very Similar to Those of *cE* and Are Omitted for Clarity)

	cE									*tE*			
	l/Å					φ/deg				φ/deg			
	b_{12}	b_{56}	b_{67}	b_{78}	b_{89}	b_{12}	b_{56}	b_{78}	b_{89}	b_{12}	b_{56}	b_{78}	b_{89}
1[a]	1.41	1.45	1.34	1.47	1.48	20	−10	−10	−33	20	−173	149	−33
2[a]	1.40	1.45	1.38	1.46	1.48	17	0	−9	−31	17	0	161	−35
3	1.40	1.45	1.35	1.48	1.48	16	53	−19	−4				
5	1.41	1.45	1.34	1.50	1.48	20	28	6	−2				

[a] The bond lengths and dihedral angles of the corresponding conformers of **1-Cl 1-OMe, 2-Cl**, and **2-OMe** are very similar.

Moreover, employing IR spectroscopy, Hayes and Timmons showed that the unsubstituted chalcone (1,3-diphenyl-prop-2-en-1-one) exists in a mixture of *ca.* 15% *tE* and 85% *cE* conformers in chloroform solution.[47] In ^{1}H NMR investigations of **1** in $CDCl_3$, a coupling of *o*-phenyl protons was only observed for H-α (CH adjacent to CO group), indicating a more stable *cE* conformation also for the donor-substituted derivative.[48] Thus, for a closer inspection of the photochemical behavior of the chalcones, only the *cE* conformer of **1** was treated theoretically and will be described in more detail below.

*The Effect of Bond Twisting on the Photophysics: The "Photochemical Spectrum" of **1***. Bond rotations in the excited state are of major importance to understand the fluorescence properties of these compounds.[16,23,43] The ground state *cE* structure of unbridged **1** is not planar but is distinguished by some twist around all single bonds (see Table 3). For a given perp-structure, the twist angles of the bonds not directly adjacent to the 90°-twisted bond are not much different from those of the planar structure, except for the b_{89} perp-structure which allows the rest of the molecular skeleton to planarize in the vicinity of bonds b_{56}, b_{67}, and b_{78}. Likewise, bond lengths are retained much the same in all perp-forms with the single bonds twisted. In contrast, the twisting around the double bond (b_{67}) causes a substantial lengthening of this bond (up to 1.41 Å) and a shortening of the adjacent single bonds down to 1.43 Å for b_{56} and 1.45 Å for b_{78}.

The energetics of the ground and excited states can be summarized in a "photochemical spectrum" (Figure 4) showing the raising and lowering of energies upon twisting successive flexible bonds in the molecule. In every case, the nature of the corresponding excited state is analyzed and the lowest states of locally excited (LE) and of biradicaloid (BR) character are reported. LE states involve transitions between orbitals located on the same fragment, while BR states involve orbitals localized on different sides of the twisted bond. BR states are often viewed as possible candidates for enhanced nonradiative deactivation because they can be located very close to a conical intersection between S_1 and S_0.[49] Here, we take a significant reduction in the S_1-S_0 energy for the Franck−Condon (FC) conformation as an indication that a conical intersection (photochemical funnel) can be reached easily through relaxation of further coordinates.[50−52]

As seen from the photochemical spectrum of **1** (Figure 4), the calculations predict an efficient "funnel" for the nonradiative degradation of the excited-state energy only for twisted double bond b_{67}, with a strong reduction of the energy gap between the ground and the lowest BR excited state down to 2.47 eV in the gas phase and expected to reduce further to 2.35 eV in a polar solvent like acetonitrile. The BR states of the other perp-structures, associated with single bond twistings, are rather high

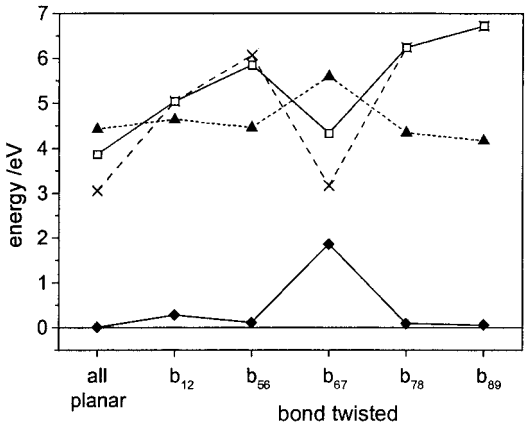

Figure 4. Ground-state and excited-state energies for **1** for the planar conformation and for various conformations with the bond indicated twisted to 90°. For numbering, see Scheme 1. Ground-state energy (solid line and diamonds) corresponds to full optimization. The lowest biradicaloid (BR) excited states are calculated for the same geometry (Franck−Condon geometries) and are labeled BR-singlet (solid line, open squares) and BR-triplet (dashed line, crosses). For comparison, the lowest locally excited state (dotted line, solid triangles) is also included.

lying in energy, especially that arising from the b_{89} twist, and are not likely candidates for nonradiative deactivation (Table 4). Noteworthy is also that the BR state involving the twisted double bond (b_{67}) perp-structure possesses a considerable singlet−triplet splitting which is attributable to some delocalization of π-orbitals over both moieties despite the twisted structure.

Table 4 and Figure 5 demonstrate that solvation effects should cause no substantial changes in the photochemical behavior of **1**, because the bond which might be most strongly responsible for a possible twist-induced funneling situation, bond b_{67}, is characterized by the smallest difference in the dipole moments between the ground and the lowest BR state ($\Delta\mu_{BR-S0} = 2.6$ D).

4. Discussion

In an interpretation of the emission behavior of the D−A−chalcones, possible deactivation routes of the initially excited singlet state including rotations around certain bonds, the electronic nature of the states populated and their dipole moment, and isomerization reactions need to be considered. Thus, to gain mechanistic access, we will leave aside the possible occurrence of different *E* conformers at first and ask the question, which of the various possible twisting coordinates will most strongly lead to a nonradiative coupling of ground and excited state. This can, for example, occur if thermally available excited state conformations are populated which possess a very narrow S_0-S_1 energy gap or are otherwise located in the neighborhood of a conical intersection. A further possibility for a strong fluorescence quenching is the coupling of S_1 and T_1 through an enhancement of intersystem crossing (ISC) for these active conformations. A well-known case for such an enhancement of nonradiative effects is connected with the proximity of $n\pi^*$ and $\pi\pi^*$ states, especially when the $n\pi^*$ state is the lowest singlet excited state.[53]

Solvatokinetic effects can help in learning something about the adiabatic photochemical reaction mechanism involved. These effects indicate how the fluorescence quenching reaction depends on solvent polarity and can therefore give an indication as to the polar properties of the species which quenches the fluorescence. In the case of the D−A-stilbenes and related

TABLE 4: Energies of the Ground and Excited States of 1 in Vacuum and the Polar Solvent Acetonitrile

	vacuum								solvent[a]		
structure	E_{S0} eV	E_{CT} eV	E_{LE} eV	ΔE_{LE-CT} eV	μ_{S0} D	μ_{CT} D	μ_{LE} D	$\Delta\mu_{CT-S0}$ D	E_{S0} eV	E_{CT} eV	E_{LE} eV
planar	0	3.86 (S_1)	4.42 (S_2)	−0.56	4.42	11.77	7.10	2.68	−0.07	3.36	4.24
b_{12}	0.28	5.04 (S_4)	4.64 (S_1)	0.4	2.99	13.76	5.02	10.77	0.25	4.35	4.55
b_{56}	0.10	5.84 (S_5)	4.45 (S_1)	1.39	4.34	14.75	8.42	10.41	0.03	5.05	4.19
b_{67}	1.85	4.32 (S_1)	5.59 (S_2)	−1.27	5.40	8.00	11.18	2.60	1.74	4.09	5.14
b_{78}	0.09	6.24 (S_1)	4.34 (S_1)	1.9	3.85	18.56	8.42	14.71	0.04	4.99	4.08
b_{89}	0.05		4.16 (S_1)		4.81		(13.54)		−0.03	0	3.49

[a] Acetonitrile; $\epsilon = 37.5$; $r = 4.71$ Å; $\rho = 0.95$ g cm^{-3}; $\epsilon_0 \approx 0.1$ (ESU cm^{-1}).

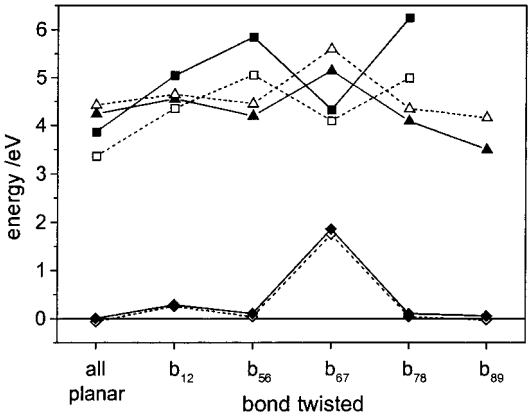

Figure 5. Energy stabilization of the ground (diamonds), TICT excited (squares), and locally excited (triangles) states. Solid and dotted lines represent state energies in the gas phase and in acetonitrile solution.

dyes,[17] e.g., a negative solvatokinetic effect was observed with quenching rates decreasing as solvent polarity increases, indicating a weakly polar biradicaloid state P* as the quenching state.[54] In the case of the dual fluorescing TICT compounds (see refs 24,43), both precursor and product state of the reaction can be observed in fluorescence, and the relative changes in fluorescence quantum yield can directly be related to a positive solvatokinetic behavior with the photochemical reaction from a less polar precursor to the highly polar TICT product being accelerated with solvent polarity.[24,55] In the chalcone case, considering at first only the compounds with similar donor−acceptor substitution pattern, we observe a positive solvatokinetic effect for the quenching reaction in **2** (reduction in solvent polarity enhances the fluorescence), but a negative solvatokinetic effect (reduction in solvent polarity quenches fluorescence) is observed for **1**, **3**, and **5** (with the exception of the region of high solvent polarity, i.e., acetonitrile for the former derivative). This directly leads to the conclusion that different quenching mechanisms are active in these two cases.

Multiple State Model. In analogy to the D−A−stilbenes,[17] we can gain access to an understanding of the photophysical behavior by using a mechanistic model which involves the all-planar excited conformation E*, the CC double bond-twisted species, with biradicaloid properties and a reduced dipole moment (P* state), and one or several C−C single bond-twisted species of highly polar nature, designated as A* state and related to the TICT mechanism.

The opposite tendencies in solvatokinetic behavior of **1**, **3**, and **5** (negative) on one hand and of **2** (positive) on the other hand directly suggest that a weakly polar, nonemissive P* state enhances the nonradiative losses in the former three compounds upon decreasing solvent polarity. Moreover, a major influence of a dimethylamino bond (b_{12}) twisting on the excited state deactivation of these chalcones can be directly excluded on the basis that qualitatively similar effects are observed for compounds **1** and **4** as well as **5** and **6**, at least for low polarities. Accordingly, the differences in the maximum of the ϕ_f vs $E_T(N)$ plot for **1** (**5**) and **4** (**6**) (Figures 2 and 3) point to a stronger charge transfer in the E* state in the latter compound with the julolidyl group as a stronger donor. A similar explanation has been given by Wang, his data being partly included in Table 1. Results published recently by Fery-Forgues et al. on benzoxazinone derivatives[56] (Scheme 3) and by Köhler et al. on D−A−stilbenes[32] (Scheme 3) point into the same direction of a stronger donor character associated with the julolidyl group. The effect of varying acceptor strength on the energetics of the excited states involved will be discussed in more detail below in combination with the applicability of the multiple state model to **1-Cl** **1-OMe**, **2-Cl**, and **2-OMe**.

Considering the anilino bond (b_{56}), the formation of a highly polar excited state (A*) can occur via twisting around b_{56}. This is possible for all compounds except for **2** and the fully bridged **8**. The highly fluorescent **7** demonstrates that any nonradiative deactivation via a possible b_{56} twisting is weak to negligible. The weak fluorescence property of **2** may therefore be related to the impossibility of populating such a fluorescent A* state. The positive solvatokinetic behavior of fluorescence quenching in **2** indicates the involvement of a quenching state of higher polarity than the precursor state E*, but it must be different from the emissive A* state (around b_{56}). This nonradiative state may be connected with twisting of the bond b_{78} connecting the heterocyclic system with the keto group. Because of its connection with CO twisting, we will call this highly polar quenching state K*, to distinguish it from the highly polar but luminescent A* state reachable by twisting the anilino bond b_{56}.

Comparing the solvent-dependent fluorescence quantum yield data of **1**−**8**, a negative solvatokinetic behavior is only observed for **1**, **3**, and **5** as well as (partly) **4** and **6** with an unbridged anilino bond, suggesting the involvement of such an A* state. Bridging of the C−C single bonds b_{78} and b_{89} as in **3** and **5** does not strongly alter the shape of the ϕ_f vs $E_T(N)$ plot (Figure 2). The curve has a similar shape but is of lower amplitude for **5** and especially for **3** as compared to **1**.[57] Accordingly, for these single bonds, two contradictory observations are made: (i) bridging the bonds adjacent to the CO group leads to increased fluorescence quenching (**3** and **5** as compared to **1**) but (ii) the lack of this bridge and the introduction of a different bridging pattern can open an efficient nonradiative funnel as well (in weakly fluorescent **2**). Thus, C−C single bond-twisted states (K*) in keto derivatives such as **2** seem to be especially weakly emissive and the larger fluorescence quantum yield of **1** can be explained as being due to the fact that an emissive A* state competes successfully with the transition to the quenching K* state. Very efficient K* state formation is known to be responsible for the weak emission of compounds related to **2** such as Michler's ketone[59] and DMABK[60] (Scheme 3). Since related D−A−stilbenes containing a central double bond fixed

SCHEME 3: Chemical Structures of the Related Benzoxazinone,[56] D−A−Stilbene,[32] and Benzofuran[61] Derivatives, Michler's Ketone,[59] DMABK,[60] and DMABI[64]

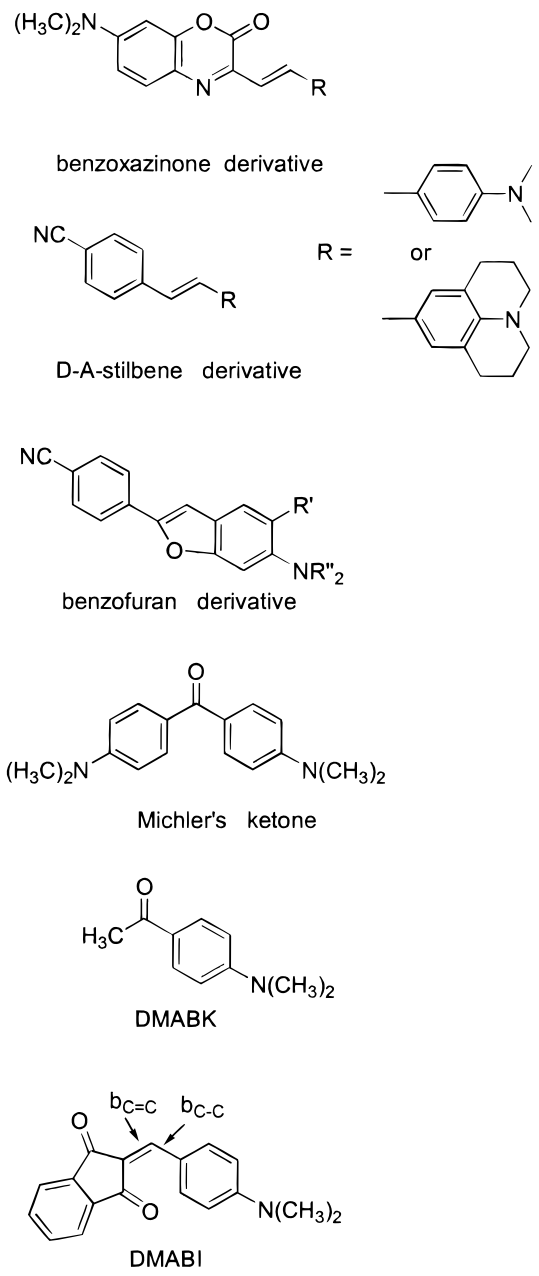

by a similar bridge as in **2** (oxygen-bridged benzofuran derivatives, Scheme 3) exhibit moderate fluorescence in polar solvents (quantum yield of 0.13 in aqueous solution[61]), no intrinsic quenching channel due to this oxygen bridge is probable. Furthermore, both bridged derivatives **7** and **8** are highly fluorescent despite an intramolecular oxygen bridge as in **2**.

The effect of donor−acceptor substitution pattern on the relative energetic position of the states P*, A*, and K* is obvious from a comparison of **1**, **1-Cl**, and **1-OMe** as well as **2**, **2-Cl**, and **2-OMe**. Increasing the acceptor strength in the unbridged derivative (**1** → **1-Cl**) shifts the maximum of the ϕ_f vs $E_T(N)$ plot to the region of lower polarity (maxima at $E_T(N) = 0.37$ for **1** and 0.33 for **1-Cl** in Figure 3[62]). In **1-Cl**, the possibility of populating the fluorescent A* state is enhanced as compared to the reaction toward the quenching state P*. Accordingly, this

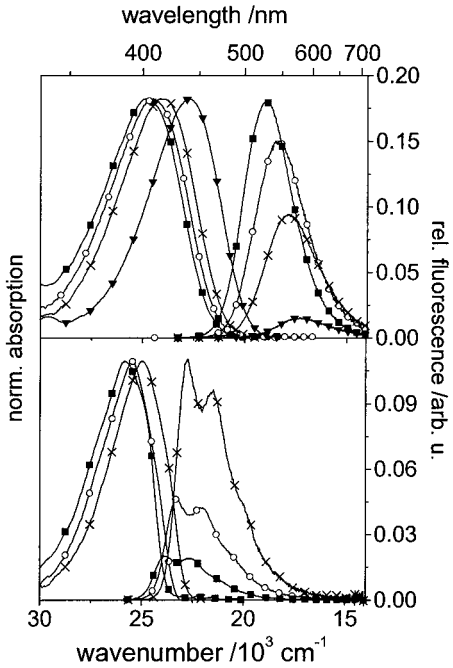

Figure 6. Normalized absorption and relative emission spectra (normalized to the same optical density at the excitation wavelength) of D−A−chalcones carrying different acceptors. Top: spectra of **1-OMe** (solid squares), **1** (open circles), and **1-Cl** (crosses) in acetonitrile; the spectra of **4** (solid triangles) in the same solvent are included for comparison. Bottom: spectra of **2-OMe** (solid squares), **2** (open circles), and **2-Cl** (crosses) in *n*-hexane.

behavior is reversed for **1-OMe**, i.e., P* and A* are closer lying in energy and the maximum of the ϕ_f vs $E_T(N)$ plot (minimum of quenching interaction by P*) is only reached in acetonitrile, the solvent of highest polarity employed (Figure 3). The competetive interaction and highly polar nature of the other quenching state(s) K* is also obvious from a comparison of the plots in Figure 3. Upon going from dichloromethane ($E_T(N) = 0.309$) to acetonitrile ($E_T(N) = 0.460$), the fluorescence losses are most pronounced for the compound with the strongest acceptor (**1-Cl**, 3.5-fold decrease in ϕ_f), less pronounced for intermediate **1** (1.6-fold) and for **1-OMe**, the opposite, i.e., an increase in fluorescence quantum yield is observed (from 0.13 to 0.18). For a better illustration of this influence of electron-donating or -withdrawing substituents, Figure 6 contains a set of spectra of **1**, **1-Cl**, and **1-OMe** in acetonitrile. As already mentioned above, the differences between **1** and **4** can be understood on this basis as well. **4**, showing bathochromically shifted spectra and a maxmium in the ϕ_f vs $E_T(N)$ plot at lower polarities than **1-Cl** ($E_T(N) = 0.28$ for **4**, Figure 3), is also the weakest emitting chalcone of the series **1**, **1-Cl**, **1-OMe**, and **4** in acetonitrile (Figure 6). The fluorescence quenching toward higher polarities producing the maximum in the ϕ_f vs $E_T(N)$ plot are due to the polar quenching state K* as discussed below.

Similar effects seem to account for the observations made for the substitution of the COPh acceptor with a *p*-Cl or *p*-OCH_3 group in bridged **2**. Increasing the strength of the CT process as in **2-Cl** leads to a higher fluorescence yield in apolar solvents. Here, initially excited, polar, and fluorescent E* is less quenched by population of nonemissive weakly polar P* as, e.g., in **2** (Figure 3). Consequently, a nonemissive highly polar K* state is already accessible in weakly or medium polar solvents such as diethyl ether or THF and the curve of **2-Cl** is already of lowest amplitude in these solvents (Figure 3). Introducing a donor group (methoxy group) in the acceptor part of **2**, a compound (**2-OMe**) with a similar behavior as observed for **4**

or **6** is obtained. For **2-OMe**, in apolar solvents the interaction of quenching mechanisms (P* state formation, proximity effect) is dominant but with increasing solvent polarity, fluorescing E* is more strongly stabilized and fluorescence is regained (maximum in the ϕ_f vs $E_T(N)$ plot in THF in Figure 3). Upon further increasing solvent polarity, the highly polar but nonemissive K* state is responsible for enhanced nonradiative deactivation. Accordingly, the influence of donor acceptor strength on the photophysical properties of the bridged derivative **2** is again well-illustrated in the lower part of Figure 6, emphasizing the apolar side of the solvent polarity range.

Returning to the comparison of **1** with **3** and **5** (where quenching via a K* state is not possible), different reactivities for nonradiative P* and luminescent A* state formation should occur. The torsion angles around b_{56} given in Table 2 are much larger in the case of the two bridged derivatives and thus not only population of a fluorescent A* state but also reaction toward a nonemissive P* state might be accelerated.[63] Even in the case of related DMABI (Scheme 3), where donor and acceptor moiety are nearly planar in the ground state, Gulbinas et al. recently attributed efficient P* state formation ($b_{C=C}$, see Scheme 3) to be responsible for the generally weak fluorescence of this dye molecule ($\phi_f < 0.01$ throughout the solvent polarity region from *n*-hexane to DMSO) despite possible population of an A* state (b_{C-C}, see Scheme 3).[64]

Nonradiative Behavior in Alkanes. In apolar solvents such as *n*-hexane, formation of a weakly polar P* state alone cannot explain the decrease in fluorescence quantum observed for most of the compounds regardless of the bridging pattern in the ϕ_f vs $E_T(N)$ plot (Figures 2 and 3). Most probably, in these solvents, the emitting polar state is sufficiently destabilized to experience perturbation by the proximity effect, i.e., vibronic coupling to energetically close lying $n\pi^*$ states.[53]

Conformational Isomerism. In the following subsection, the implications of the multiple state model will be examined more closely for their consistency with the stereoisomerism of the D−A−chalcones. The only two derivatives fixed in the *tE* conformation are the highly fluorescent and largely bridged **7** and **8**. Here, in apolar solvents, mainly the proximity effect should lead to fluorescence quenching, but in all the more polar solvents, only a polar fluorescent *tE** state emits. Additionally, in the case of **7**, a highly polar, fluorescent *tA** emitting species is assumed to play a role. The higher fluorescence quantum yield of **7** as compared to **8** in acetonitrile (Figure 2),[7] the increased solvatochromic behavior found by Wang and Wu for **7**,[7] and the assignment of the fluorescence of a derivative of **7** to CT fluorescence from an emissive TICT state[65] given in the literature so far support these assumptions.

None of the compounds **3**, **5**, and **6** with a fixed *cE* conformation possesses a bridged double bond, and thus the rate of intrinsic *cE* fluorescence remains unknown. But emission in these compounds with a flexible double bond occurs most probably via A* population (aniline twisting), counterbalanced by (parallel or consecutive) reaction toward nonemissive P* (double bond twisting). This is in accord with the three-state model developed for the related D−A−stilbenes which predicts an enhancement of the nonradiative losses due to the more efficient population of the P* state in such a case of some pretwisting of the double bond.[17]

Concerning **1**, **2**, and their substituted analogues, all able to adopt the *cE* and/or the *tE* conformation, the ground state equilibrium between both conformers will be largely dependent on their stabilization by the respective solvent. Upon increasing solvent polarity, the conformer with the higher dipole moment will be more strongly stabilized. If both ground state conformers are present, the excited-state reaction scheme extends to a dual scheme with individual species *tA**, *cA**, *tP**, and *cP** (Scheme 4). However, the close spectroscopic relation of both *E* conformers is exemplified by the spectrally similar absorption and emission characteristics of, e.g., **5** (fixed *cE*) and **8** (fixed *tE*) and is supported by the quantum chemical calculations.

SCHEME 4: Generalized Excited State Reaction Model for D−A−Chalcones (Triplet States, Reverse Reactions, and Consecutive Population of Two Excited Species are Omitted for Clarity)[a]

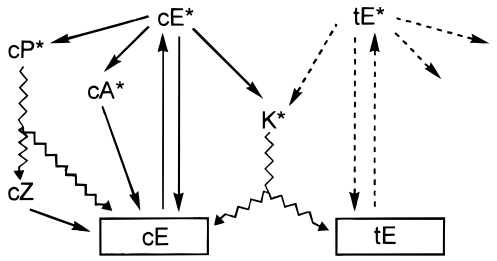

[a] Dashed arrows indicate the second branch, coming into play when both ground state conformers *tE* and *cE* are excited. Solid arrows denote reactions and radiative deactivations, and wiggled arrows mark nonradiative decays. Any triplet formation would occur most probably from P*.

The large difference in fluorescence quantum yields between **1**−**6** and **7** and **8** in any solvent or medium of high polarity demonstrates the efficient population of nonemissive K* and P* states. But whereas the conical intersection responsible for the P* type funnel is well approximated by the twist of the double bond in the quantum chemical calculations, the behavior connected with the formation of K* is not well reproduced. Here, the one-dimensional approach employed in the calculations apparently fails to model the actual molecular changes sufficiently well and additional coordinates are required to describe this conical intersection.[51,52,66] Future work using the phase change rule[51,52] may help to identify the missing coordinates. This paper is meant to pave the way and establish experimental facts.

Triplet Formation. With the data given in the results section, the role of triplet state population cannot be elucidated any further in this paper. However, intersystem crossing should occur most probably from P*. In the case of the related bis(*p*-(dimethylamino)benzylidene)acetone, DeVoe et al. found direct experimental evidence for the formation of a "dark" P* state by employing transient absorption spectroscopy.[4] The lack of the detection of any photoproducts in these studies,[4] neither by addition reactions nor by trans−cis isomerization,[67] and the energetically unstable *Z* conformers (any species formed by C=C double bond twisting should undergo a very rapid backward reaction leading to the ground state *E* conformer) do not point to a major contribution of intersystem crossing for the deactivation of excited 4′-(dimethylamino)chalcones.

5. Conclusion

The fluorescence efficiencies of chalcones with various bridged bonds and different donors and acceptors can be understood by considering (at least) four photophysically active states: the highly emissive all-planar structure E*, a further emissive and highly polar state of twisted structure (A*, probably involving the twist of the anilino group), and two nonemissive states of low (P*, twisting of the double bond) and high dipole moment (K*). The quantum chemical calculations support the identification of P* with a twist of bond b_{67}

and suggest that it corresponds to a structure not far from a conical intersection. From the experimental bridging studies, K* is related with the twisting of the ketone function (b_{78}), but the calculations do not indicate a significant S_0/S_1 narrowing as expected for the approach to a conical intersection. This might be due to the involvement of a second coordinate to reach the conical intersection[66] which has not been considered in these one-dimensional calculations. The nature of this second coordinate remains to be determined. Recent qualitative improvement in the understanding of conical intersections by the phase change rule[51,52] should be a promising approach to solving this question.

Acknowledgment. Financial support by the Deutsche Forschungsgemeinschaft (DFG; Re 387/8-2 and Re 387/13-1) and the Bundesministerium für Bildung und Forschung (BMBF, 13N7120) is gratefully acknowledged.

References and Notes

(1) Nicodem, D. E.; de M. G. Matos, J. A. *J. Photochem.* **1981**, *15*, 193.
(2) Caldwell, R. A.; Singh, M. *J. Am. Chem. Soc.* **1983**, *105*, 5139.
(3) Wang, Y. *J. Phys. Chem.* **1985**, *89*, 3799.
(4) DeVoe, R. J.; Sahyun, M. R. V.; Schmidt, E.; Sadrai, M.; Serpone, N.; Sharma, D. K. *Can. J. Chem.* **1989**, *67*, 1565.
(5) Gustav, K.; Bartsch, U.; Karnizschky, K. *Z. Chem.* **1989**, *29*, 213.
(6) Jiang, Y.-B.; Wang, X.-J.; Lin, L. *J. Phys. Chem.* **1994**, *98*, 12367.
(7) Wang, P.; Wu, S. *J. Photochem. Photobiol. A: Chem.* **1995**, *86*, 109.
(8) Su, G.-B.; He, Y.-P.; Li, Z.-D. *Jiegou Huaxue (Chinese J. Struct. Chem., Engl. Transl.)* **1997**, *16*, 263.
(9) Mager, L.; Melzer, C.; Barzoukas, M.; Fort, A.; Mery, S.; Nicoud, J.-F. *Appl. Phys. Lett.* **1997**, *71*, 2248.
(10) Monroe, B.; Smothers, W. K.; Keys, D. E.; Krebs, R. R.; Mickish, D. J.; Harrington, A. F.; Schicker, S. R.; Armstrong, M. K.; Chan, D. M. T.; Weathers, C. I. *J. Imaging Sci.* **1991**, *35*, 19.
(11) Rurack, K.; Bricks, J. L.; Kachkovskii, A. D.; Resch, U. *J. Fluoresc.* **1997**, *7*, 63S. Rurack, K.; Bricks, J. L.; Slominskii, J. L.; Resch-Genger, U. In *Near-Infrared Dyes for High Technology Applications*; Dähne, S., Resch-Genger, U., Wolfbeis, O. S., Eds.; Kluwer Academic: Dordrecht, 1998; p 191.
(12) Rurack, K.; Bricks, J. L.; Radeglia, R.; Resch-Genger, U. *J. Phys. Chem. A*, submitted.
(13) Lewis, G. N.; Calvin, M. *Chem. Rev.* **1939**, *25*, 273. Hofer, L. J. E.; Grabenstetter, R. J.; Wiig, E. O. *J. Am. Chem. Soc.* **1950**, *72*, 203.
(14) Carstens, T.; Kobs, K. *J. Phys. Chem.* **1980**, *84*, 1871.
(15) Jones, II, G.; Jackson, W. R.; Choi, C.-Y.; Bergmark, W. R. *J. Phys. Chem.* **1985**, *89*, 294.
(16) Létard, J.-F.; Lapouyade, R.; Rettig, W. *J. Am. Chem. Soc.* **1993**, *115*, 2441.
(17) Rettig, W.; Majenz, W.; Herter, R.; Létard, J.-F.; Lapouyade, R. *Pure Appl. Chem.* **1993**, *65*, 1699.
(18) Lapouyade, R.; Czeschka, C.; Majenz, W.; Rettig, W.; Gilalbert, E.; Rullière, C. *J. Phys. Chem.* **1992**, *96*, 9643.
(19) Sczepan, M.; Rettig, W.; Bricks, Y. L.; Slominski, Y. L.; Tolmachev, A. I. *J. Photochem. Photobiol. A: Chem.* **1999**, *124*, 75.
(20) Vogel, M.; Rettig, W. *Ber. Bunsen-Ges. Phys. Chem.* **1985**, *89*, 962.
(21) Vogel, M.; Rettig, W.; Sens, R.; Drexhage, K. H. *Chem. Phys. Lett.* **1988**, *147*, 452.
(22) Vogel, M.; Rettig, W.; Sens, R.; Drexhage, K. H. *Chem. Phys. Lett.* **1988**, *147*, 461. Vogel, M.; Rettig, W.; Fiedeldei, U.; Baumgärtel, H. *Chem. Phys. Lett.* **1988**, *148*, 347.
(23) Plaza, P.; Dai Hung, N.; Martin, M. M.; Meyer, Y. H.; Vogel, M.; Rettig, W. *Chem. Phys.* **1992**, *168*, 365.
(24) Grabowski, Z. R.; Rotkiewicz, K.; Siemiarczuk, A.; Cowley, D. J.; Baumann, W. *Nouv. J. Chim.* **1979**, *3*, 443. Rettig, W. *Angew. Chem., Int. Ed. Engl.* **1986**, *25*, 971. Rettig, W. In *Modern Models of Bonding and Delocalization*; Liebman, J. F., Greenberg, A., Eds.; VCH: New York, 1988; p 229.
(25) Drexhage, K. H. *J. Res. Natl. Bur. Stand. (U.S.)* **1976**, *80A*, 421.
(26) Resch, U.; Rurack, K. *Proc. SPIE-Int. Soc. Opt. Eng.* **1997**, *3105*, 96.
(27) Sachs, F.; Lewin, W. *Ber.* **1902**, *35*, 3569.
(28) Grosscurt, A. C.; Van Hes, R.; Wellinga, K. *J. Agric. Food Chem.* **1979**, *27*, 406.
(29) Tewari, R. S.; Dubey, A. K.; Misra, N. K. *J. Chem. Eng. Data* **1981**, *26*, 106.
(30) Zubarovskii, V. M.; Bricks, J. L. *Ukr. Khim. Zh.* **1982**, *48*, 761. Zubarovskii, V. M.; Bricks, J. L. *Khim. Heterocycl. Soed.* **1982**, *N5*, 644.
(31) Shriner, R. L.; Teeters, W. O. *J. Am. Chem. Soc.* **1938**, *60*, 936.
(32) Rechthaler, K.; Köhler, G. *Chem. Phys. Lett.* **1996**, *250*, 152.
(33) Dewar, M. J. S.; Zoeblich, E. G.; Healy, E. F.; Stewart, J. J. P. *J. Am. Chem. Soc.* **1985**, *107*, 3202.
(34) Dewar, M. J. S.; Stewart, J. J. P.; Ruiz, J. M.; Liotard, D.; Healy, E. F.; Dennington, R. D., II *AMPAC 4.5* and *AMPAC 5.0*; Semichem: Shawnee, 1993 and 1994.
(35) Létard, J.-F.; Lapouyade, R.; Rettig, W. *Chem. Phys.* **1994**, *186*, 119.
(36) Onsager, L. *J. Am. Chem. Soc.* **1936**, *58*, 1486.
(37) Böttcher, C. J. F. *Theory of Electric Polarization*, 2nd ed.; Elsevier: Amsterdam, 1973; Vol. 1.
(38) Karelson, M.; Zerner, M. C. *J. Am. Chem. Soc.* **1990**, *112*, 9405.
(39) Bilot, L.; Kawski, A. *Z. Naturforsch.* **1962**, *17a*, 621.
(40) Varma, C. A. G. O.; Groenen, E. J. J. *Recl. Trav. Chim. Pays-Bas* **1972**, *91*, 296.
(41) Hansch, C.; Leo, A.; Taft, R. W. *Chem. Rev.* **1991**, *91*, 165.
(42) Dimroth, K.; Reichardt, C.; Siepmann, T.; Bohlmann, F. *Justus Liebigs Ann. Chem.* **1963**, *661*, 1.
(43) Rettig, W. *Top. Curr. Chem.* **1994**, *169*, 253.
(44) In polar protic solvents (alcohols), the fluorescence of all D−A−chalcones (note that no data are available for **7** and **8**) is drastically quenched as a consequence of hydrogen bond formation at the carbonyl group in the acceptor part.[3,45]
(45) Inoue, H.; Hida, M.; Nakashima, N.; Yoshihara, K. *J. Phys. Chem.* **1982**, *86*, 3184.
(46) Rabinovich, D. *J. Chem. Soc. B* **1970**, 11. Rabinovich, D.; Schmidt, G. M. J.; Shaked, Z. *J. Chem. Soc., Perkin Trans. 2* **1973**, 33.
(47) Hayes, W. P.; Timmons, C. J. *Spectrochim. Acta* **1968**, *24A*, 323.
(48) Rurack, K.; Radeglia, R. Unpublished results.
(49) Michl, J. *J. Mol. Photochem.* **1972**, 243 and 257. Michl, J. *Pure Appl. Chem.* **1975**, *41*, 507. Michl, J. *Top. Curr. Chem.* **1974**, *46*, 1. Zimmerman, H. E. *J. Am. Chem. Soc.* **1966**, *88*, 1566. Bonacic-Koutecký, V.; Michl, J. *J. Am. Chem. Soc.* **1985**, *107*, 1765. Michl, J.; Bonacic-Koutecký, V. *Electronic Aspects of Organic Photochemistry*; J. Wiley & Sons: New York, 1990. Bernardi, F.; Olivucci, M.; Robb, M. A. *J. Photochem. Photobiol. A: Chem.* **1997**, *105*, 365. Celani, P.; Bernardi, F.; Olivucci, M.; Robb, M. A. *J. Chem. Phys.* **1995**, *102*, 5733.
(50) Fuss, W.; Lochbrunner, S.; Müller, A. M.; Schikarski, T.; Schmid, W. E.; Trushin, S. A. *Chem. Phys.* **1998**, *232*, 161. Garavelli, M.; Vreven, T.; Celani, P.; Bernardi, F.; Robb, M. A.; Olivucci, M. *J. Am. Chem. Soc.* **1998**, *120*, 1285.
(51) Zilberg, S.; Haas, Y. *J. Phys. Chem. A* **1999**, *103*, 2364.
(52) Zilberg, S.; Haas, Y. *Chem.—Eur. J.* **1999**, *5*, 1755.
(53) Wassam, W. A., Jr.; Lim, E. C. *J. Chem. Phys.* **1978**, *68*, 433.
(54) Rettig, W.; Majenz, W. *Chem. Phys. Lett.* **1989**, *154*, 335.
(55) Hicks, J.; Vandersall, M.; Babarogic, Z.; Eisenthal, K. B. *Chem. Phys. Lett.* **1985**, *116*, 18. Rettig, W. In *Dynamics and Mechanisms of Photoinduced Electron Transfer and Related Phenomena*; Mataga, N., Okada, T., Masuhara, H., Eds.; Elsevier: Amsterdam, 1992; p 57.
(56) Fery-Forgues, S.; Le Bris, M. T.; Pouget, J.; Rettig, W.; Valeur, B. *J. Phys. Chem.* **1992**, *96*, 701.
(57) The generally lower fluorescence quantum yield in the case of **3** can be understood on the basis of the higher flexibility of the cyclohexene ring undergoing a nearly barrierless ring inversion (boat−chair interconversion).[58]
(58) Jensen, F. R.; Bushweller, C. H. *J. Am. Chem. Soc.* **1969**, *91*, 5774.
(59) Lippert, E.; Rettig, W.; Bonacic-Koutecký, V.; Heisel, F.; Miehé, J. A. *Adv. Chem. Phys.* **1987**, *68*, 1.
(60) Kirkor-Kaminska, E.; Rotkiewicz, K.; Grabowska, A. *Chem. Phys. Lett.* **1978**, *58*, 379.
(61) Grynkiewicz, G.; Poenie, M.; Tsien, R. Y. *J. Biol. Chem.* **1985**, *260*, 3440.
(62) Maximum of a third-order polynomial fit of the ϕ_f vs $E_T(N)$ plot.
(63) The excited-state reaction mechanism might as well involve reactions between states (e.g., P* and A*) which are not discussed here any further.
(64) Gulbinas, V.; Kodis, G.; Jursenas, S.; Valkunas, L.; Gruodis, A.; Mialocq, J.-C.; Pommeret, S.; Gustavsson, T. *J. Phys. Chem. A* **1999**, *103*, 3969.
(65) Revill, J. A. T.; Brown, R. G. *J. Fluoresc.* **1992**, *2*, 107. Revill, J. A. T.; Brown, R. G. *Chem. Phys. Lett.* **1992**, *188*, 433.
(66) Longuet-Higgins, H. C. *Proc. R. Soc. London, Ser. A* **1975**, *344*, 147. Herzberg, G.; Longuet-Higgins, H. C. *Trans. Faraday Soc.* **1963**, *35*, 77.
(67) Photochemical products have only been reported for the unsubstituted parent compound 1,3-diphenylprop-2-en-1-one[1] and for bis(*p*-(dimethylamino)benzylidene)acetone.[4]
(68) Lippert, E. *Z. Elektrochem.* **1957**, *61*, 962.